International Journal of Applied Mathematics

Volume 36 No. 4 2023, 437-453

ISSN: 1311-1728 (printed version); ISSN: 1314-8060 (on-line version)

doi: http://dx.doi.org/10.12732/ijam.v36i4.1

IDENTIFICATION OF PRESTRESS IN INHOMOGENEOUS VISCOELASTIC TIMOSHENKO PLATES

Ivan V. Bogachev ¹, Mikhail I. Chebakov ¹, Maria D. Datcheva ^{2,§}

¹I. I. Vorovich Institute of Mathematics Mechanics and Computer Sciences Southern Federal University Rostov-on-Don – 344000, RUSSIAN Federation ² Institute of Mechanics Bulgarian Academy of Sciences Sofia – 1113, BULGARIA

Abstract: Proceeding from the general theory of steady-state vibrations of inhomogeneous prestressed bodies, in the present work the problem of bending vibrations of circular and annular inhomogeneous plates is considered within the framework of Timoshenko's hypotheses, taking into account the viscoelastic (rheological) properties of the material. The material rheology is described by the three-parameter viscoelastic Zener type model (also known as the Standard Linear Solid model) employing instantaneous and long-term constitutive moduli, as well as the relaxation time. For the formulation of the governing equations the Volterra correspondence principle and the concept of complex modules were used. For the both types of plates, a method is proposed for solving the corresponding direct (forward) problems for determining the vibrations using a weak formulation, based on the Galerkin method, and taking into account that the functions involved are complex-valued.

The proposed method is verified by a comparison of the results of calculating the plate deflection with the analytical solution in the case of homogeneous prestressed plates. The influence of the prestress level on the amplitude-frequency characteristics is analyzed in order to identify the most effective modes of acoustic sounding.

Received: June 23, 2023 © 2023 Academic Publications

Furthermore, a new formulation of the inverse problem is proposed to identify the prestress in inhomogeneous viscoelastic plates using the information on the acoustic response of the plate. To solve the formulated inverse problem, a modification of the previously developed special projection approach is used, whose applicability is illustrated by a set of numerical experiments. The influence of input data noise on the prestress identification accuracy is also analyzed.

AMS Subject Classification: 74D99

Key Words: prestressed state, inhomogeneous plates, Timoshenko's model, viscoelasticity, acoustic methods, inverse analysis

1. Introduction

New functionally graded and composite materials, including polymer composites, with a complex inhomogeneous structure are nowadays used in many areas of modern technology and production (see, for example, review paper [1], in particular, in aircraft engineering [2], space technologies, for development of "smart" systems as well as for prosthetics in medicine. The properties of such materials can vary significantly in the sample volume, while due to inhomogeneity and complex rheology, the direct experimental evaluation of these properties requires significant material costs and time resources. At the same time, when modeling the behavior of such materials, one must take into account the presence in a large part of structural elements made of modern functionally graded materials of a prestress field (PSF) [3]-[4], which has a significant impact on the functionality and serviceability of the final product. The presence of prestress is related to the specificity of the production technological process [5], including various types of heat treatments, polymerization, crystallization and cooling of the products, as well as creep and relaxation, which are associated with viscoelastic materials [6]. Prestress is quite common in polymer composites [7], which are produced by autoclave technology followed by solidification of the resulting material. This technology, on the one hand, allows to avoid the appearance of microdefects, cracks and delamination in the composite; on the other hand, residual stresses and strains occur during the manufacturing process, which significantly affect the mechanical characteristics of the compos-[8], [9]. In this regard, the design of adequate models that describe the behavior of the material, taking into account the existing heterogeneity and the possible presence of prestress, as well as the development of easy-to-apply effective non-destructive methods for identifying the level of prestress and its

distribution, are of particular importance. Currently, there is an intensive development of experimental methods for measuring prestress, which is reflected in a large number of recent publications (see, for example, reviews [3], [10]). Widespread among them are the methods that are designed for objects made of composite materials, in particular plate structures, which structures are also the subject of the present study. In [11], a method was proposed for measuring tensile stresses that occur at the interfaces between materials in composite three-layer plates during gas tungsten arc welding. The article [12] reports results from a simulation of the residual stresses that occur during the production by the layer-by-layer photopolymerization method using 3D printing. It has been shown there that exceeding the prestress level leads to a significant deviation of products' shape from the set one. Therefore, it is necessary to optimize the technological process, and in the given article, staged photopolymerization with stress control at each stage is proposed. In [13] it is presented an analytical solution to the two-dimensional problem of fabricating a heavy semicircular arch from prestressed viscoelastic aging material. In addition, the presence of residual stresses has been shown to reduce the contact stresses at the base of the structure, which provides greater stability compared to non-prestressed structural elements. The article [14] presents a specific methodology for determining prestresses and residual strains in composite automotive parts, which is based on a combination of finite element modeling and the method of thermal analysis and drilling holes. This methodology allows for long-term prediction of the behavior of the manufactured parts during their operation. Drilling holes to determine the prestresses was also used in [15] for polycarbonate samples, where it was concluded that the resistance of polycarbonate to cracking increases when certain compressive stress fields are created in it. The article [16] presents a method for estimating the distribution of thermal stresses occurring during a laminated ceramic disc manufacturing. The study was carried out using finite element modeling, further investigating the effect of porosity on the residual stresses in the ceramic laminate, which revealed a decrease in the level of residual stresses with increasing porosity. Regarding the modeling of polymer composites, it should be noted the finite ABAQUS, used for example in [17] to simulate the residual stress that occurs during curing of viscoelastic composites employing the generalized Maxwell viscoelasticity model with n elements. A similar study to determine the effect of compressive prestresses on the behavior of viscoelastic polymer matrix composites was conducted in [18]. Another practical application of models for prestressed composite materials is in the study of polymer pipes, for which stresses arising during their operation affect their service life. An example of such a study can be found in

[19], where the results of finite element modeling were compared with experimental studies of polyethylene samples of different brands, which allowed to develop criteria for evaluating the residual life of pipes. Thus, we can conclude that the modeling of composite materials in which there are residual stresses as well as the identification of the presence of such are very important tasks that have a focus on various practical applications. It is also worth noting that a number of inverse problems similar to those considered in this paper for identifying inhomogeneous prestress fields in plates and other bodies have also been investigated previously [20], [21], [22]. In [21], inverse problems for the identification of prestress fields occurring in bending vibrations of plates were studied. The analysis is done within the framework of Timoshenko's hypotheses, using several techniques based on the acoustic approach. Models of circular elastic inhomogeneous prestressed Timoshenko plates were developed in [22] and the problem of identifying the prestresses was solved using the projection approach allowing to determine the desired characteristics in the given classes of functions.

This paper presents an extension of the models within Timoshenko's hypotheses for stationary bending vibrations of circular and annular inhomogeneous plates with consideration of residual stresses, as well as of the methods for solving the problem of identifying residual stresses based on acoustic sounding data proposed in [22], to the case of plates made of composite materials that possess viscoelastic (rheological) properties.

2. Problem formulation

The problem of a Timoshenko viscoelastic plate vibrations is formulated here adopting the linearized formulation of the problem of stationary vibrations of a prestressed anisotropic viscoelastic body [20]. It is considered a plate composed of a material of density $\rho(x, y, z)$ enclosed by a surface $S = S_u \cup S_\sigma$. At the boundary S_u , the plate is fixed, and at the boundary S_σ it is loaded with a periodic load with angular velocity ω and components of the loading vector $P_i e^{-i\omega t}$. The corresponding equations of motion and boundary conditions read:

$$\begin{split} T_{ij,j} + \rho \omega^2 u_i &= 0, \\ T_{ij} &= \sigma_{ij} + u_{i,n} \sigma_{nj}^0, \\ T_{ij} n_j |_{S_{\sigma}} &= P_i, \quad u_i |_{S_u} = 0, \end{split} \tag{1}$$

where u_i are the components of the displacement vector, σ_{ij} are the components of the symmetric Kirchhoff stress tensor, σ_{ij}^0 are the components of the prestress tensor, T_{ij} are the components of the Piola unsymmetrical stress.

According to the elastic–viscoelastic correspondence principle, the constitutive relations are given as:

$$\sigma_{ij} = G_{ijkl}(\omega)u_{k,l}, \qquad (2)$$

where the components of the complex module G_{ijkl} describe the viscoelastic behavior of the material according to the standard Zener model [7], and are expressed as:

$$G_{ijkl}(\omega) = \frac{-E_{ijkl}ni\omega + H_{ijkl}}{-ni\omega + 1}.$$
 (3)

The model is a 3-parameter model with H_{ijkl} – long-term modules, E_{ijkl} – instantaneous modules ($E_{ijkl} > H_{ijkl} > 0$) and n > 0 – relaxation time.

Furthermore, based on (1)–(2), we formulate the problem of steady-state axisymmetric bending vibrations of circular and annular (with inner radius R_0) viscoelastic inhomogeneous prestressed plates with radius R and thickness h in a cylindrical coordinate system (r, φ, z) . According to Timoshenko's theory, the corresponding assumptions for the components of the displacement vector have the form:

$$u_r = z\theta, \quad u_\varphi = 0, \quad u_z = w, \tag{4}$$

where w is the plate deflection, θ is the angle of rotation of the normal along the axis of the radial coordinate. The vibrations are caused by an applied normal load q(r) ($P_i = q$, i = 1, 2, 3).

For convenience and brevity, the following notations are used $r = R\xi$, w = $R\tilde{w}, G = G_0\tilde{G}, R_0 = R\xi_0, G_0 = G(R,0), , \sigma_{rr}^0 = \frac{12G_0}{h^3}s_{rr}^0, \rho = \rho_0(R)\tilde{\rho},$ $\kappa^2 = \frac{h^3\rho_0}{12G_0}R^2\omega^2, q = \frac{12G_0}{h^2R}\tilde{q}(\xi), \gamma = 12\frac{R^2}{h^2}.$ The case of a plane prestress state is considered [23], in which the only nonzero stress components $\sigma_{rr}^0(r) \neq 0$ and $\sigma_{\varphi\varphi}^0(r) \neq 0$ are satisfying the Cauchy equilibrium equation $\sigma_{rr}^{0'} + \frac{\sigma_{rr}^0 - \sigma_{\varphi\varphi}^0}{\xi} = 0$, hence $\sigma_{\varphi\varphi}^0 = \xi \sigma_{rr}^{0'} + \sigma_{rr}^0$. In the modeling hereafter, we proceed from the situation that is quite common in practice, when it is required to determine the prestresses in viscoelastic bodies after a considerable time has passed since the removal of the impact that caused them, see e.g. [19]. In this case, the current prestress state can be considered independent of time and the ongoing relaxation is very slow compared to the speed of the processes occurring during the excitation of vibrations. Consequently, the prestress practically do not change with time and are considered functions of spatial coordinates only. The correctness of this assumption is illustrated in [24], where prestresses occurring in a viscoelastic material during stress relaxation is considered. It is shown there that for a considerable time after the application of the initial load or strain, the prestresses are real functions of the coordinates.

According to the correspondence principle, we write the equations of vibrations of the considered prestressed plates under conditions (4), using the equations obtained in [22] for the elastic case, written in terms of dimensionless parameters and variables:

$$\left(\xi \left[G\frac{(1-\nu)}{2}\left(\theta+w'\right)+s_{rr}^{0}w'\right]\right)'-\kappa^{2}\rho\xi w+q\xi=0,$$

$$\gamma\xi \left[G\frac{(1-\nu)}{2}\left(\theta+w'\right)+s_{rr}^{0}w'\right]-\left(\xi \left[G\left(\theta'+\frac{\nu\theta}{\xi}\right)+s_{rr}^{0}\theta'\right]\right)'$$

$$+G\left(\nu\theta'+\frac{\theta}{\xi}\right)+\frac{\left(\xi s_{rr}^{0}'+s_{rr}^{0}\right)\theta}{\xi}-\kappa^{2}\rho\xi\theta=0.$$
(5)

In equations (5), instead of the function of the cylindrical stiffness of the plate $D(r) = \frac{E(r)h^3}{12(1-\nu^2)}$ used in the elastic case [22] (where E(r) is the Young's modulus and ν is the Poisson's ratio), the complex modulus function of the form (3) is used, i.e. $G(\xi, i\kappa) = \frac{i\tau\kappa g_2(\xi)+g_1(\xi)}{1+i\tau\kappa}$. In addition, in formulas (5), the tilde character is omitted, and the derivative with respect to the dimensionless coordinate ξ is indicated by apostrophe. The plate deflection function $w(\xi, \kappa)$ and the angle $\theta(\xi, \kappa)$ of rotation of the normal in the considered case are complex and the density ρ is a function solely of the dimensionless radius ξ .

We assume that the plates are tightly fasten along the outer contour, which is expressed by the following boundary conditions:

$$w(1,\kappa) = 0, \quad \theta(1,\kappa) = 0. \tag{6}$$

The additional boundary conditions are as follows. For the circular plate due to symmetry we have:

$$w'(0,\kappa) = 0, \quad \theta(0,\kappa) = 0.$$
 (7)

The annular plate is considered to be also fixed along the inner boundary:

$$w(\xi_0, \kappa) = 0, \quad \theta(\xi_0, \kappa) = 0. \tag{8}$$

For the boundary value problems (5)-(6),(7) and (5)-(6),(8) we formulate the inverse problems to identify the prestress distribution based on periodic acoustic load. The inverse problem consists in determining the dimensionless prestress real function $s_{rr}^0(\xi)$ from additional information about the deflection of the plates measured at the acoustic sounding location $\xi = \xi_z$ in a given frequency range:

$$w(\xi_z, \kappa) = f(\kappa), \quad \kappa \in [\kappa_1, \kappa_2].$$
 (9)

The other mechanical characteristics of the plates are known. The formulated inverse problems for determining the prestress fields are nonlinear and

ill-posed problems [25], which requires a specific approach to finding the solution.

3. Plate vibrations and dynamic characteristics analysis

In the present work, due to the nonlinearity of equations (5), a technique based on the Galerkin numerical method was used to solve the forward problem of calculating the bending vibrations of the considered prestressed viscoelastic plates. For this, we use the weak formulation of both problems by projecting equations (5) onto the fields of possible deflections w_1 and rotation angles θ_1 . Performing simple transformations and using the boundary conditions (6) as well as (7) for the solid circular plate and (8) for the annular plate, we end with:

$$\int_{\xi_{0}}^{1} \left(\gamma \xi \theta_{1} \left(G \frac{(1-\nu)}{2} + s_{rr}^{0} \right) w' + \left(\left(\gamma \xi G \frac{(1-\nu)}{2} + \frac{G + \xi \sigma_{rr}^{0} + \sigma_{rr}^{0}}{\xi} - \kappa^{2} \rho \xi \right) \theta_{1} - G \nu \theta_{1}' \right) \theta - \left(\xi \left(G + s_{rr}^{0} \right) \theta_{1}' - G \nu \theta_{1} \right) \theta' \right) \xi d\xi = 0,$$

$$\int_{\xi_{0}}^{1} \left(\xi \left(G \frac{(1-\nu)}{2} + s_{rr}^{0} \right) w_{1}' w' + G \frac{(1-\nu)}{2} \xi w_{1}' \theta - \kappa^{2} \rho \xi w_{1} w \right) \xi d\xi = - \int_{\xi_{0}}^{1} q \xi^{2} w_{1} d\xi.$$
(10)

In (10) for the case of solid circular plate, $\xi_0 = 0$.

Then we express the complex-valued functions of the deflection and the angle of rotation of the normal in the form of the following expansions in terms of basis functions $\varphi_{1m}(\xi)$, $\varphi_{2m}(\xi)$ that satisfy the main boundary conditions:

$$w(\xi,\kappa) = \sum_{m=1}^{N} a_m(\kappa)\varphi_{1m}(\xi), \ \theta(\xi,\kappa) = \sum_{m=1}^{N} b_m(\kappa)\varphi_{2m}(\xi).$$
 (11)

The basis functions for the solid circular plate are chosen as:

$$\varphi_{1m}(\xi) = (1 - \xi^2)^2 \xi^{2(m-1)}, \ \varphi_{2m}(\xi) = \sin(m\pi\xi).$$
(12)

The basis functions for the angular plate are:

$$\varphi_{1m}(\xi) = (1 - \xi^2)^2 (\xi - \xi_0)^2 \xi^{2(m-1)}, \ \varphi_{2m}(\xi) = \sin\left(m\pi \frac{\xi - \xi_0}{1 - \xi_0}\right).$$
 (13)

The coefficients $a_m(\kappa)$ and $b_m(\kappa)$ are complex function of frequency.

Afterwards, expressions (11) are put into (10) and the basis functions $w_1 = \varphi_{1m}(\xi)$, $\theta_1 = \varphi_{2m}(\xi)$, m = 1, ..., N, of the form (12) or (13), respectively, are chosen as possible functions. As a result, the forward problems are reduced to solving the system of linear equations of dimension 2N with respect to the coefficients $a_m(\kappa)$ and $b_m(\kappa)$ for the chosen values of the dimensionless vibration frequency κ .

The above technique is verified by applying it to the vibration analysis of homogeneous plates and comparing the obtained solutions with the analytical ones expressed with Bessel functions. Below are the results of the comparison of the analytical and numerical solutions. For a solid circular plate, Figure 1 shows the results of calculating the deflection function (a) and the normal rotation angle function (b); while for the annular plate, the results are shown in Figure 2. In both figures, the solid line indicates the analytical solution, the dots indicate the numerical solution. The deviation when choosing 7 basis functions was less than 2%, when choosing 10 - less than 1%, which indicates a fairly high accuracy of the proposed here solution technique.

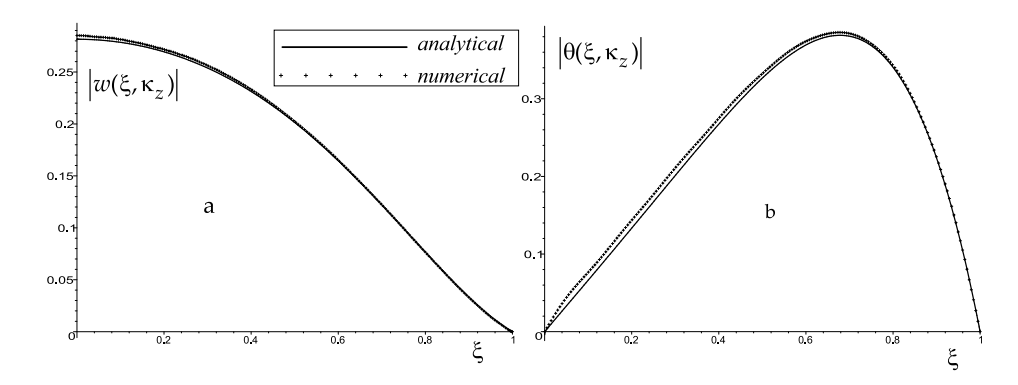


Figure 1: Comparison of the analytical (solid line) and numerical (dots) solutions to the problem of calculating the deflection functions (a) and the normal rotation angle (b) of a solid circular plate.

For both cases – solid circular and annular plates – a set of numerical experiments was carried out to calculate the amplitude–frequency characteristics in the vicinity of the first dimensionless frequency of viscoelastic resonance (extremum) for different prestress levels, predetermined by the level of dimensionless initial load p_0 ($p_0 = 10^{-3}, ..., 10^{-2}$) and the zero value in the absence of prestress. In the problem for the solid circular plate, a uniform prestress field was chosen corresponding to the solution of the problem of planar vibrations of a plate [23], while for the annular plate (with $\xi_0 = 0.2$), the solution of the cor-

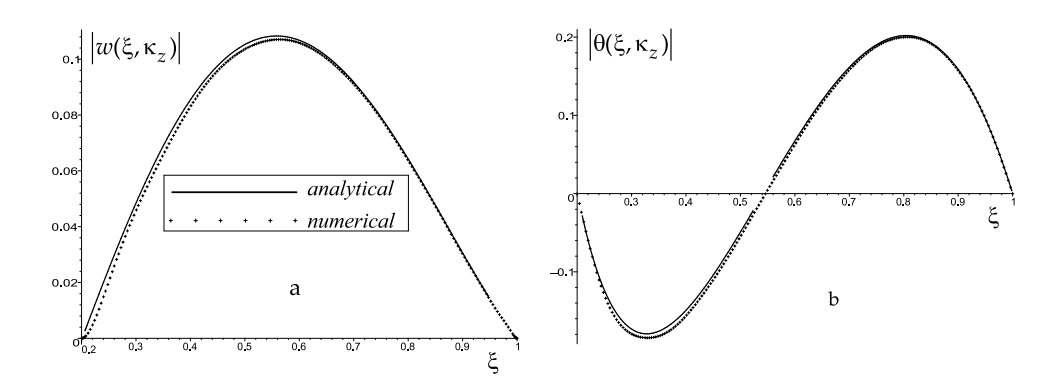


Figure 2: Comparison of the analytical (solid line) and numerical (dots) solutions to the problem of calculating the deflection functions (a) and the normal rotation angle (b) of an annular plate.

responding Lame problem for a ring [26] loaded by a latent internal pressure, the form of which is given below with Eq. (17). The results of experiments on calculating the modulus of the complex-valued frequency response at the probing point for the solid circular and annular plates are shown in Figure 3(a, b), respectively. In all figures, the solid line marks the solutions of the problem at $p_0 = 0$ (no prestress), the dotted lines are for the values of the dimensionless prestress values $p_0 = 10^{-3}$, $5 \cdot 10^{-3}$, 10^{-2} .

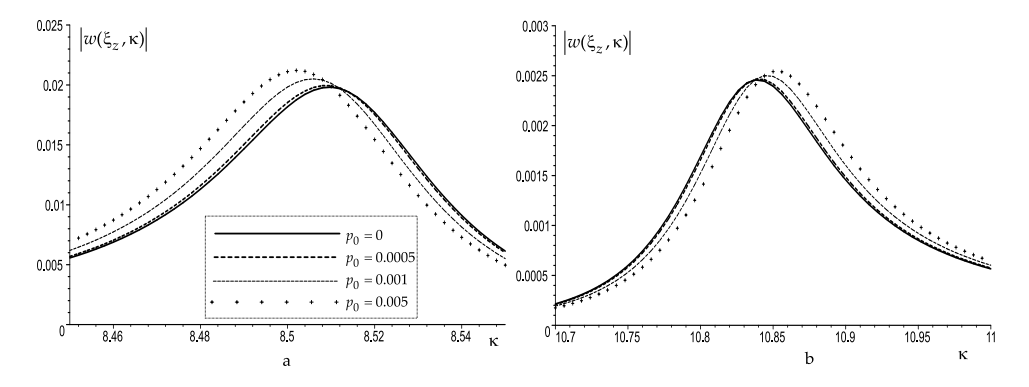


Figure 3: Influence of the prestress level on the frequency response of solid circular (a) and annular (b) plates in the vicinity of the first viscoelastic resonance.

As in previous studies for elastic plates and other objects, the results of

numerical experiments show that the differences in frequency response are most pronounced near the frequencies of the viscoelastic resonance.

4. Inverse problem's solution strategy

To solve the corresponding inverse problems, we used an adapted projection method, described earlier in [27], based on the representation of all unknown functions as expansions of linearly independent functions and using the weak formulation (10). For the plate deflection functions $w(\xi,\kappa)$ and the angle of rotation of the normal $\theta(\xi,\kappa)$, we use expansions of the form Eq. (11), with basis functions (12) and (13), respectively. Within the framework of this method, the prestress $s_{rr}^0(\xi)$ is also expanded in terms of a system of linearly independent functions:

$$s_{rr}^{0}(\xi) = \sum_{j=1}^{M} C_{j} \psi_{j}(\xi). \tag{14}$$

Further, as in the approach for solving the forward problems, we form a system of linear equations with respect to the coefficients in expansions (11), then, choosing M frequencies κ_m , from the conditions (9) we obtain systems of M nonlinear equations of order 2M with respect to the set of real coefficients C_j of the expansions (14):

$$w(\xi_z, \kappa_m, C_j) = f(\kappa_m), \ j = 1, ..., M, \ m = 1, ..., M.$$
 (15)

The Newton method was used to solve these systems of nonlinear equations. As a result of calculating the coefficients C_j , the function $s_{rr}^0(\xi)$ is determined in the form (14).

It has to be noted that for solving the system (15) in the considered here viscoelastic case, when the deflection and the angle of rotation of the normal are complex-valued functions, it is required rather large computing power compared to the elastic case, when these functions are real-valued. The use of the developed here approach is illustrated in detail by numerical experiments in the next section.

5. Verification via numerical experiments

Next, we present the results of numerical experiments on the use of the projection technique described in the previous section to solve the formulated inverse

No	p_0	Back-calculated val-	Back-calculated values/
		ues/ exact input	noisy input (error)
		(error)	
1	0.01	0.0010039 (0.03%)	0.0009928 (1.11%)
2	0.005	0.0050067 (0.13%)	0.0050701 (1.40%)
3	0.001	0.0009933 (0.66%)	0.0009627 (3.72%)

Table 1: Identification of the prestress for a solid circular viscoelastic plate for exact and noisy input data

problems for identifying the plane prestress distribution $s_{rr}^0(\xi)$ in viscoelastic plates. In the first two experiments, the back-calculation of the prestresss that arose during the initial radial loading of the plates with a normal load p_0 applied on the outer boundary in the case of a solid circular plate, and on the inner boundary in the case of the annular plate, is presented. In this particular case, the distribution of the radial stresses in the solid circular plate is constant [23]:

$$s_{rr}^{0}(\xi) = p_0. (16)$$

In the case of annular plate, the radial stresses can be defined as a solution to the corresponding Lame problem for a disk [26]:

$$s_{rr}^{0}(\xi) = \frac{p_0}{\xi_0^{-2} - 1} \left(1 - \frac{1}{\xi^2} \right). \tag{17}$$

Note that in both cases the prestress is predetermined by the initial load parameter p_0 to which the developed here technique is applied. Moreover, in the expansion (14) it is used one basis function of type (16) or (17), respectively, and a single value of the sensing frequency.

Experiment 1. Determination of different prestress values in the solid circular plate, caused by a normal load p_0 (homogeneous prestress field) with sensing sound frequencies near the first resonance $\kappa=8.45$. Table 1 shows the results from the numerical experiment both for exact and for noisy input data. The introduced noise of 0.5% significantly exceeds the error of modern devices used in the implementation of the acoustic methods. For the back-calculated values of the prestress, the identification error is indicated in parentheses.

Experiment 2. Determination of the initial loading parameter p_0 , which caused in the anular plate a prestress of the type (17). The results are presented in Table 2 for both exact and 0.5% noisy input data.

No	p_0	Back-calculated val-	Back-calculated values/
		ues/ exact input	noisy input (error)
		(error)	
1	0.01	$0.0099734 \ (0.26\%)$	0.0009750 (2.5%)
2	0.005	0.0049842 (0.31%)	0.0049473 (3.13%)
3	0.001	0.0009961 (0.38%)	0.0011214 (12.15%)

Table 2: Identification of the prestress level in an annular viscoelastic plate based on exact and noisy input data

Note that, as for elastic plates, with a decrease in the prestress level, its effect on the frequency response decreases, and therefore the accuracy of its determination worsen. Below are the results of using the developed here methodology in numerical experiments to determine arbitrary prestress values, whose origin is generally unknown (it can be initial elastic/ plastic deformation, temperature or other effects, and their combinations). On the graphs illustrating the results of the back-calculations, the solid line indicates the desired function, the dots indicate the back-calculated function.

Experiment 3. It is considered a case of initial elastic deformation of an annular plate of radius $\xi_0=0.2$, due to a pressure $p_0=10^{-3}$ at the inner boundary. In this case, the prestress distribution reads $s_{rr}^0(\xi)=\frac{p_0}{\xi_0^{-2}-1}\left(1-\frac{1}{\xi^2}\right)$. The frequency range [9.2, 9.3] is chosen for the identification procedure. The back-calculation was carried out in the class of linear functions $(M=2,\psi_j(\xi)=\xi^{j-1})$ and in Figure 4(a) are shown the results. When trying to back-calculate the presress in of type (17), the function can be restored almost exactly. The result is shown in Figure 4(b).

Experiment 4. The numerical experiment is a model case. The task is to reconstruct the increasing quadratic function $s_{rr}^0(\xi)=10^{-3}(1+\xi^2)$ in case of solid circular plate in the frequency range [7.8, 8.1] and within the class on the linear function $(M=2,\psi_j(\xi)=\xi^{j-1})$. Figure 5 shows the result from the back-calculation procedure.

Experiment 5. This numerical experiment is a model case. It is an application of the proposed here identification technique to back-calculate of signalternating functions describing the prestress field (e.g., compressive prestress within one part of the plate, and tension prestress within the other). For the solid circular plate, the decreasing prestress function $s_{rr}^0(\xi) = 10^{-3} \cdot (0.5 - \xi^2)$ was considered, while for the annular plate, the increasing one $s_{rr}^0(\xi) = 10^{-3} \cdot (0.5 - \xi^2)$. The identification procedure was carried out in the class of linear

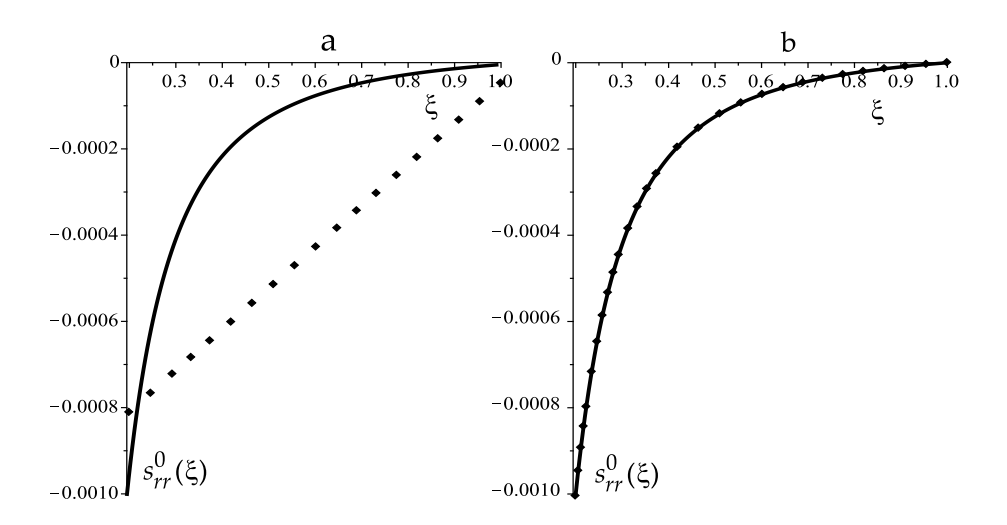


Figure 4: Reconstruction of the prestress distribution function for an annular plate in the case of elastic deformation. Inverse modelling within the class of linear functions - (a), in the form (17) - (b).

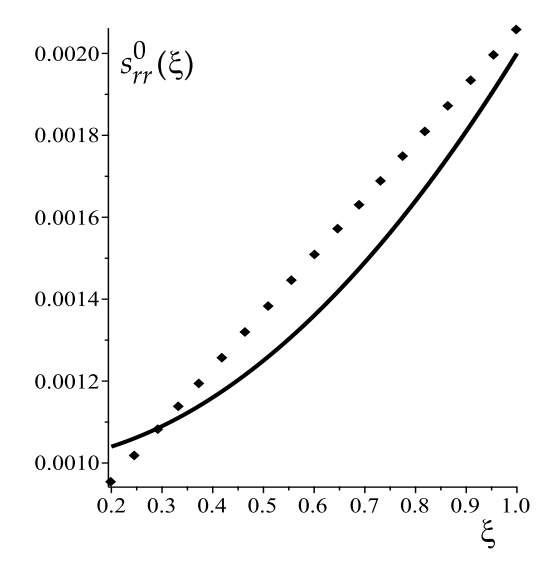


Figure 5: Reconstruction of the prestress distribution function for a solid circular plate (Experiment 4).

functions $(M=2,\psi_j(\xi)=\xi^{j-1})$. Figure 6 depicts the results of the back-calculation carried out (the back-calculation is almost exactly recovering the forward problem input data).

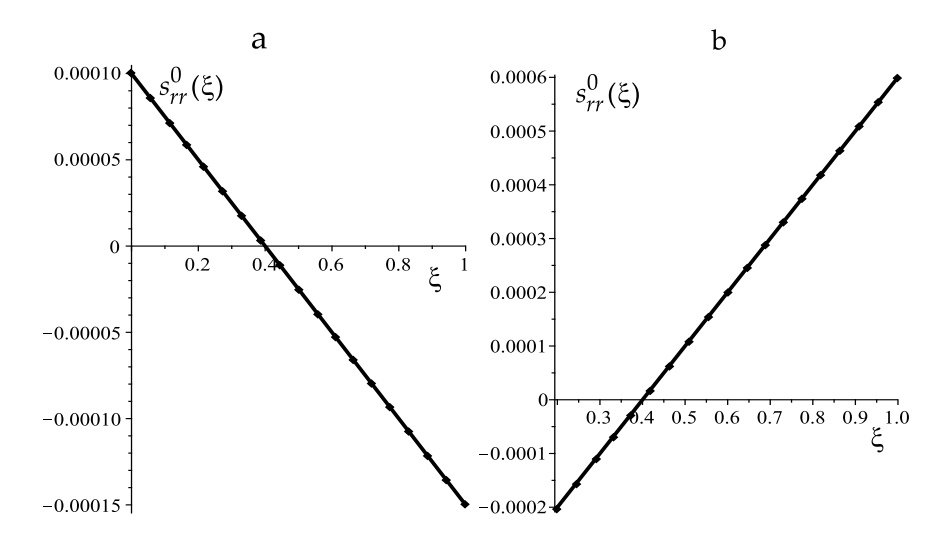


Figure 6: Reconstruction of alternating prestress distribution functions for (Experiment 5). For a solid circular plate – (a), for annular plate – (b).

It has to be noted that from a practical point of view, the prestress identification within the class of linear functions can be considered the most promising, since real prestress distribution functions in plates are most often monotonic and the actual task is to determine the prestress level and the nature of its monotonicity. Also, this approach is the most efficient in terms of speed, taking into account the need to solve cumbersome systems of linear and nonlinear equations with complex coefficients.

6. Conclusion

To solve the inverse problems of identifying the prestress in solid circular and annular inhomogeneous round viscoelastic Timoshenko plates when considering bending vibrations, a special projection technique was adapted to implement the acoustic approach. Additional studies have been carried out to provide practical recommendations for achieving the best quality of reconstruction; the results of numerical experiments on solving the corresponding inverse problems, carried out using these recommendations, are presented. The technique has

shown its applicability for the prestress identification, both in the case when the prestress nature of occurrence is known, and for arbitrary cases. It is also applicable for noisy input data.

Acknowledgements. This study was carried out with the financial support of the Ministry of Science and Higher Education of the Russian Federation (State task in the field of scientific activity, scientific project No. FENW-2023-0012) (M. Chebakov & I. Bogachev) and the Bulgarian National Science Fund under the grant KP-06 Russia/5 (M. Datcheva).

References

- [1] H.S. Mali, P. Sharma, Machinability of high-strength fiber-reinforced polymer textile composites: a review, *Mech. Compos. Mater.*, **59** (2023), 1-28.
- [2] S.B. Sapozhnikov, M.Y. Semashko, A.N. Shanygin, Measurement of hoop strength in wound composite ring specimen using modified split disk test, *Mech. Compos. Mater.*, **59** (2023), 77-88.
- [3] G.S. Schajer, *Practical Residual Stress Measurement Methods*, John Wiley & Sons, New York (2013).
- [4] N.S. Rossini, M. Dassisti, K.Y. Benyounis, A.G. Olabi, Methods of measuring residual stresses in components, *Materials and Design*, **35** (2012), 572-588.
- [5] B. Kieback, A. Neubrand, H. Riedel, Processing techniques for functionally graded materials, *Materials Science and Engineering: A*, 362 (2003), 81-106.
- [6] J.D. Ferry, Viscoelastic Properties of Polymers, John Wiley & Sons, New York (1980).
- [7] R.M. Christensen, *Mechanics of Composite Materials*, John Wiley & Sons, New York (1979).
- [8] E.N. Kablov, V.O. Startsev, The influence of internal stresses on the aging of polymer composite materials: A review, *Mech. Compos. Mater.*, **57** (2021), 565-576.
- [9] V.L. Bogdanov, On one approach in fracture mechanics of composites with parallel cracks under the action of initial (residual) stresses, *Mech. Compos. Mater.*, **59** (2023), 239-262.

- [10] J. Guo, H. Fu, B. Pan, R. Kang, Recent progress of residual stress measurement methods: a review, *Chinese Journal of Aeronautics*, 2 (2021), 54-78.
- [11] N. Li, M. Zhang, J.-L. Ye, C. Liu, Experimental investigation on residual stress distribution in zirconium/titanium/steel tri-metal explosively welded composite plate after cutting and welding of a cover plate, *Journal of Manufacturing Proc.*, **64** (2021), 55-63.
- [12] P.S. Bychkov, V.M. Kozintsev, A.V. Manzhirov, A. L. Popov, Determination of residual stresses in products in sdditive production by the layer-by-layer photopolymerization method, *Mechanics of Solids*, 52, No 5 (2017), 524-529.
- [13] A.V. Manzhirov, D.A. Parshin, Application of prestressed structural elements in the erection of heavy viscoelastic arched structures with the use of an additive technology, *Mechanics of Solids*, 51, No 6 (2016), 692-700.
- [14] A.V. Kim, D.A. Kim, H.J. Oh, S.H. Lee, J. R. Youn, Residual stresses and viscoelastic deformation of an injection molded automotive part, *Korea-Australia Rheology Journal*, 19, No 4 (2007), 183-190.
- [15] A. Magnier, B. Scholtes, T. Niendorf, On the reliability of residual stress measurements in polycarbonate samples by the hole drilling method, *Polymer Testing*, 71 (2018), 329-334.
- [16] I.Y. Smolin, V.A. Zimina, S.P. Buyakova, Estimation of residual thermal stresses in a layered ceramic composite, *Mech. Compos. Mater.*, **58** (2023), 823–834.
- [17] A. Ding, S. Li, J. Wang, L. Zu, A three-dimensional thermo-viscoelastic analysis of process-induced residual stress in composite laminates, *Com*posite Structures, 129 (2015), 60-69.
- [18] B. Wang, K. Fancey, Viscoelastically prestressed polymeric matrix composites: an investigation into fibre deformation and prestress mechanisms, Composites Part A: Applied Science and Manufacturing, 111 (2018), 106-114.
- [19] J. Poduška, P. Hutař, J. Kučera, A. Frank, J. Sadílek, G. Pinter, L. Náhlík, Residual stress in polyethylene pipes, *Polymer Testing*, 54 (2016), 288-295.

- [20] I.V. Bogachev, A.O. Vatulyan, V.V. Dudarev, R.D. Nedin, The investigation of the initial stress-strain state influence on mechanical properties of viscoelastic bodies, PNRPU Mechanics Bulletin, 2 (2019), 15-24.
- [21] R.D. Nedin, A.O. Vatulyan, I.V. Bogachev, Direct and inverse problems for prestressed functionally graded plates in the framework of the Timoshenko model, *Math. Meth. Appl.*, 41, No 4 (2018) (2018), 1600-1618.
- [22] I.V. Bogachev, Determination of prestress in circular inhomogeneous solid and annular plates in the framework of the Timoshenko hypotheses, Applied Sciences, 11 (2021), 9819.
- [23] Yu.A. Amenzade, Theory of Elasticity, Mir Publishers, Moscow (1979).
- [24] I.V. Bogachev, R.D. Nedin, On characteristic identification for prestressed human skin, *Russian Journal of Biomechanics*, **25**, No 3 (2021), 331-342.
- [25] A.N. Tikhonov, V.Ya. Arsenin, Methods of Solution of Ill-Posed Problems, Nauka, Moscow (1979).
- [26] A.I. Lurie, Theory of Elasticity, Springer, Berlin (2005).
- [27] A.O. Vatulyan, I.V. Bogachev, The projection method for identification of the characteristics of inhomogeneous solid, *Doklady Physics*, **63**, No 2 (2018), 82-85.